



# Metabolic Switching of *Mycobacterium tuberculosis* during Hypoxia Is Controlled by the Virulence Regulator PhoP

Prabhat Ranjan Singh,<sup>a</sup> Anil Kumar Vijjamarri,<sup>a\*</sup>  Dibyendu Sarkar<sup>a</sup>

<sup>a</sup>CSIR-Institute of Microbial Technology, Chandigarh, India

**ABSTRACT** *Mycobacterium tuberculosis* retains the ability to establish an asymptomatic latent infection. A fundamental question in mycobacterial physiology is to understand the mechanisms involved in hypoxic stress, a critical player in persistence. Here, we show that the virulence regulator PhoP responds to hypoxia, the dormancy signal, and effectively integrates hypoxia with nitrogen metabolism. We also provide evidence to demonstrate that both under nitrogen limiting conditions and during hypoxia, *phoP* locus controls key genes involved in nitrogen metabolism. Consistently, under hypoxia a  $\Delta$ *phoP* strain shows growth attenuation even with surplus nitrogen, the alternate electron acceptor, and complementation of the mutant restores bacterial growth. Together, our observations provide new biological insights into the role of PhoP in integrating nitrogen metabolism with hypoxia by the assistance of the hypoxia regulator DosR. The results have significant implications on the mechanism of intracellular survival and growth of the tubercle bacilli under a hypoxic environment within the phagosome.

**IMPORTANCE** *M. tuberculosis* retains the unique ability to establish an asymptomatic latent infection. To understand the mechanisms involved in hypoxic stress which play a critical role in persistence, we show that the virulence regulator PhoP is linked to hypoxia, the dormancy signal. In keeping with this, *phoP* was shown to play a major role in *M. tuberculosis* growth under hypoxia even in the presence of surplus nitrogen, the alternate electron acceptor. Our results showing regulation of hypoxia-responsive genes provide new biological insights into role of the virulence regulator in metabolic switching by sensing hypoxia and integrating nitrogen metabolism with hypoxia by the assistance of the hypoxia regulator DosR.

**KEYWORDS** hypoxia regulator, *M. tuberculosis* PhoP, metabolic switching, protein-protein interactions, virulence regulator

A hallmark of tuberculosis (TB) is the unique ability of *Mycobacterium tuberculosis* to establish an asymptomatic latent infection and persist within granulomas in a dormant form, sometimes for a very long time, before reactivation to cause the active disease. Since survival and persistence in this environment depend on the sensing of signals and ability to induce a robust adaptive response, one of the major aspects to understand latent TB relates to the mechanism of adaptation of the tubercle bacilli in response to environmental stress.

Despite its requirement of oxygen for growth, *M. tuberculosis* can survive during latency without oxygen for a surprisingly long time. Thus, two *in vivo* conditions are often linked to latent TB. These are hypoxia and exposure to immune effectors such as nitric oxide (NO) (1–3). The ability to produce reactive nitrogen species by host-inducible nitric oxide synthase (iNOS) contributes to TB infections by its effect on both the host and the pathogen (4). Therefore, functional iNOS expression could be detected in the lung macrophages of human TB patients (5, 6). Consistently, hypoxia and nitric oxide-dependent bacterial adaptation to a dormant state induce latent TB in mice (1,

**Citation** Singh PR, Vijjamarri AK, Sarkar D. 2020. Metabolic switching of *Mycobacterium tuberculosis* during hypoxia is controlled by the virulence regulator PhoP. *J Bacteriol* 202:e00705-19. <https://doi.org/10.1128/JB.00705-19>.

**Editor** Michael J. Federle, University of Illinois at Chicago

**Copyright** © 2020 American Society for Microbiology. All Rights Reserved.

Address correspondence to Dibyendu Sarkar, [dibyendu@imtech.res.in](mailto:dibyendu@imtech.res.in).

\* Present address: Anil Kumar Vijjamarri, National Institute of Child Health and Human Development, National Institutes of Health, Bethesda, Maryland, USA.

**Received** 15 November 2019

**Accepted** 6 January 2020

**Accepted manuscript posted online** 13 January 2020

**Published** 11 March 2020

3). During limiting oxygen concentrations, *M. tuberculosis* induces reduction of nitrate ( $\text{NO}_3^-$ ) to nitrite ( $\text{NO}_2^-$ ) to control redox homeostasis and energy production (7). When nitrate is taken up by mycobacteria via passive diffusion (8, 9), the mycobacterial nitrate reductase (encoded by *narGHIJ*) is expressed at a low level under aerobic conditions (7). Also, hypoxia promotes induction of NarK2, a nitrate transporter enabling rapid accumulation of nitrite by *M. tuberculosis* cultures growing under oxygen-limiting conditions but in the presence of nitrate (8). Consistent with these results, transcripts from *narG*, encoding a nitrate reductase subunit, and *narX*, encoding a nonfunctional nitrate reductase, were identified within granulomas of human TB samples (10, 11). These results suggest that intracellular mycobacteria within the human host encounter a very low oxygen tension and most likely adapt to the microenvironment by respiring nitrate. However, the key regulators that connect hypoxia and nitrogen metabolism of mycobacteria and that define the mechanisms that promote and maintain TB latency in humans remain poorly understood.

Previous studies have shown that upon exposure to hypoxia, carbon monoxide or nitric oxide, the *dosR-dosS* system activates expression of ~48 genes that are part of the dormancy survival (Dos) regulon (12–14). Although DosR is essential for mycobacterial survival under dormancy (12, 15), phosphorylated DosR induces the expression of hypoxia-responsive genes (13). DosR cooperatively binds to target promoters containing a minimum of two tandem binding sites, and the proximal DosR binding site often juxtaposes with the –35 sequence element of the promoters (16, 17). In keeping with this, DosR-SigA interaction remains essential in the dormancy survival program of *M. tuberculosis* (18). Although previous studies suggest that *dosR* is regulated by PhoP (19–21) via recruitment of the regulator within the *dosR* promoter region (22–24), the role of PhoP during mycobacterial hypoxia remains unknown.

Recently, Voskuil and coworkers have shown that acidic conditions of growth significantly inhibited anaerobic survival of a  $\Delta dosR$  mutant (25). However, an alkaline growth environment improved the mutant's survival. Because PhoP controls pH-driven adaptations of *M. tuberculosis* (26–29), in this study we investigated whether the virulence-associated *phoP* locus is linked to the hypoxic response of the tubercle bacilli. Transcript profiling indicates that induction of *dosR* regulon was subdued in  $\Delta phoP$  mutant, suggesting that PhoP functions as an activator of hypoxia-inducible genes. We provide evidence showing a striking increase in nitrate and nitrite reduction under hypoxia (7), a state related to nonreplicating persistence of *M. tuberculosis* either for redox balance maintenance or to provide energy during shift-down (8), is controlled by the *phoP* locus. In keeping with these results, *phoP* strongly impacts the expression of genes related to nitrogen metabolism and under oxygen austerity even in the presence of surplus nitrogen conditions the *M. tuberculosis*  $\Delta phoP$  strain was significantly growth defective relative to the wild-type (WT) bacilli. Together, these results establish that (i) metabolic switching of *M. tuberculosis* under hypoxia is achieved by integration of hypoxia with nitrogen metabolism and (ii) the convergence of PhoP and DosR as coactivators of hypoxia-inducible genes, controlled by protein-protein contacts, coordinates nitrogen metabolism in response to hypoxia.

## RESULTS

***phoP* impacts hypoxia-inducible gene expression of *M. tuberculosis*.** To investigate whether *phoP* impacts hypoxia, we compared the expression levels of hypoxia-inducible genes in WT and  $\Delta phoP$  mutant *M. tuberculosis* strains using an *in vitro* model of hypoxia (3) (Fig. 1). The results suggest that under normal conditions the major hypoxia-inducible genes, which belong to the *dosR* regulon (12, 13, 15), are significantly downregulated in the  $\Delta phoP$  mutant relative to the WT bacilli. However, during hypoxia their expressions remain comparable in the WT and the mutant strain (compare Fig. 1A and B). In contrast, *dosR* regulon genes which are involved in  $\text{N}_2$  metabolism (30) show a *phoP*-dependent activation both under normal conditions and during hypoxia (Fig. 1). Because *narG* and *nirB* control the reduction of nitrate and nitrite, respectively (30) and hypoxia is accompanied by an increase in nitrate reduction (7), these results together

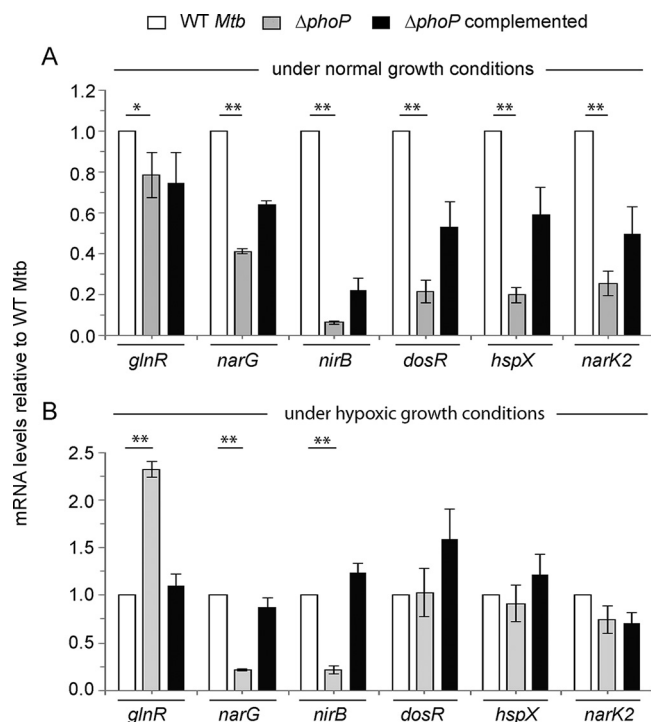


**FIG 1** *M. tuberculosis* *phoP* regulates expression of hypoxia-responsive genes *in vivo*. Real-time RT-qPCR was carried out to determine relative expression levels of indicated hypoxia-inducible genes in WT (wild-type),  $\Delta phoP$ , and complemented mutant strains both under normal conditions (A) and hypoxia (B), as described in Materials and Methods. The fold differences in mRNA levels with standard deviations from replicate experiments were determined from at least three independent RNA preparations (\*\*,  $P < 0.01$ ; \*,  $P < 0.05$ ). Mtb, *M. tuberculosis* (in this and subsequent figures).

suggest that during hypoxia PhoP appears to activate expression of genes involved in  $N_2$  metabolism. In keeping with these results, *glnR*, a major regulator of nitrate assimilation (30), is strongly repressed by PhoP during hypoxia but not under normal conditions (compare Fig. 1A and B). Although GlnR is known for its role in the nitrate assimilation of *M. tuberculosis* (30), repression of *glnR* by PhoP during hypoxia rules out the possibility of activation of *narG* and *nirB* via GlnR. Table S1 in the supplemental material lists the PAGE-purified oligonucleotides used in reverse transcription-PCR (RT-PCR) experiments. Although a previous study by Smith and coworkers had identified PhoP-regulated transcriptome, DNA arrays using exponentially growing cells under normal conditions did not reveal an influence of PhoP on the expression of *dosR* or other hypoxia-inducible genes (31). In contrast, using a different *phoP* mutant strain, Gonzalo-Asensio et al. showed that PhoP functions as an activator of *dosR* (20). Although different experimental conditions and various quantitative approaches appear to account for this discrepancy, clearly our results are consistent with those of Gonzalo-Asensio et al. showing a significant effect of PhoP on the expression of *dosR*. More recently, Vashist et al. have shown that PhoP functions as a repressor of *dosR* (24). Although both our study and this report have investigated the regulation of *dosR* by PhoP, the use of laboratory-attenuated *M. tuberculosis* H37Ra, a different genetic background comprising a genomic copy of a mutant PhoP (S219L) by Vashist et al., versus the clean mutant used in our study most likely accounts for this discrepancy. Also, it should be noted that except for PhoP binding to *nirB* promoter in a genome-wide SELEX experiment (32), there has been no new report linking PhoP with hypoxia-inducible genes other than *dosR* itself.

Next, to investigate the expression levels of *glnR*, *narG*, and *nirB*, we grew WT *M. tuberculosis* in Dubos medium with either limiting (1 mM) or surplus nitrogen (30 mM) conditions (see Fig. S1 in the supplemental material), as described earlier (33). Although

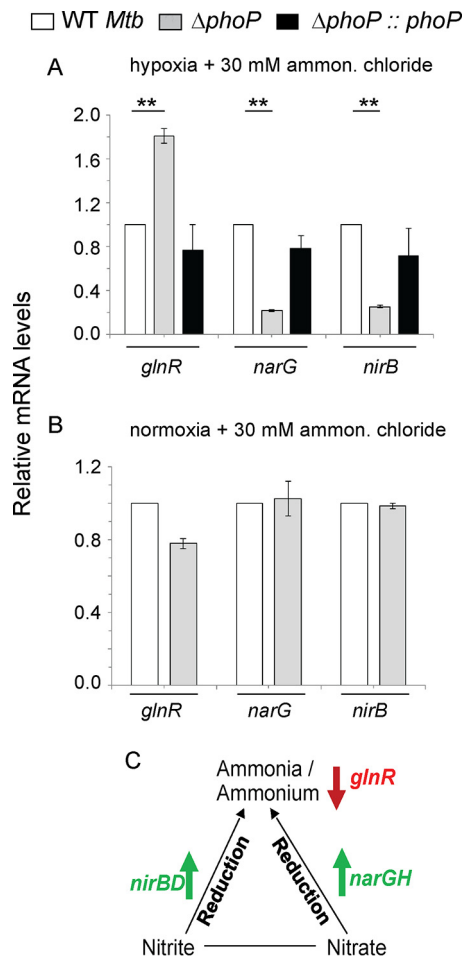


**FIG 2** Regulation of genes related to nitrogen metabolism by the *phoP* locus. (A and B) RT-qPCR was carried out to compare expression levels of hypoxia-inducible genes in the WT,  $\Delta phoP$ , and complemented mutant strains under specific and indicated conditions of growth. The differences in mRNA levels with the standard deviations were determined from at least three independent RNA preparations (\*\*,  $P < 0.01$ ). (C) Scheme summarizing *phoP*-dependent regulation of nitrogen metabolism during hypoxia. While PhoP acts as an activator of nitrite and nitrate reductases (*nirB* and *narG*, respectively) during hypoxia (as shown by upward arrows), repression of *glnR* (as shown by a downward arrow) signifies lower scavenging of nitrogen source under oxygen austerity.

mycobacterial genes involved in  $N_2$  metabolism showed a relatively lower level of expression under hypoxia coupled with limiting ammonium chloride concentration (Fig. S1A), these genes displayed a significant induction during hypoxia coupled with surplus nitrogen (Fig. S1B). In sharp contrast, regardless of the ammonium chloride concentration, the mycobacterial genes *dosR*, *hspX*, and *nark2* showed a significantly higher expression level under normoxia (compare Fig. S1A and B). It should be noted that hypoxic growth conditions in WT *M. tuberculosis* alone were unable to induce the expression of *narG* and *nirB*. However, the *dosR* regulon is strongly induced under hypoxia, showing activation of *dosR* expression (Fig. S1A). In sharp contrast, *narG* and *nirB* show a striking activation only when hypoxia is coupled with an excess of  $N_2$  source (Fig. S1B), clearly suggesting that activation of *narG* and *nirB* in *M. tuberculosis* is not attributable to hypoxia-dependent DosR activation alone.

To examine whether PhoP controls expression of mycobacterial  $N_2$  metabolism, we grew WT and  $\Delta phoP$  *M. tuberculosis* strains in Dubos medium under either limiting nitrogen (1 mM) or a nitrogen surplus (30 mM) conditions (Fig. 2). In agreement with the results presented above (Fig. 1), during hypoxia coupled with surplus nitrogen concentration, the expression of *glnR* was significantly higher in the  $\Delta phoP$  mutant,

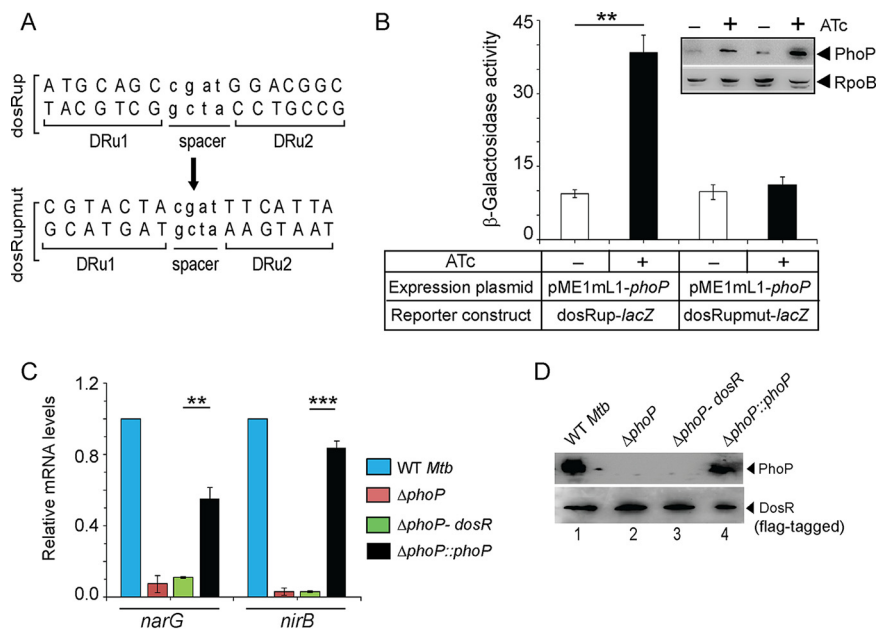


**FIG 3** Regulatory mechanism of hypoxia-inducible promoter activity by PhoP. (A) PhoP binding direct repeat motif showing upstream (DRu1) and downstream (DRu2) repeat units. The mutant promoter of *dosR* carrying changes only at the PhoP binding site, dosRupmut, was generated by changing A's to C's and G's to T's (of both repeat units) and vice versa. Next, the orientation of the DRu2 sequence was reversed relative to DRu1. (B) *M. smegmatis* strains harboring either WT (dosRup-*lacZ*) or the mutant promoter (dosRupmut-*lacZ*) construct, along with PhoP expression plasmid (pME1mL1-*phoP*), were grown for 24 h in absence (–) or presence (+) of ATc, as an inducer of PhoP expression. The  $\beta$ -galactosidase activities were determined as described in Materials and Methods. The activities represent averages of multiple experiments with standard deviations from at least three independent cultures. The inset compares the expression of PhoP in  $\sim 10 \mu\text{g}$  crude extracts as detected by anti-PhoP antibody; RpoB was used as the loading control. (C) FLAG-tagged DosR was cloned and expressed in mycobacterial expression vector p19Kpro (54) as described in Materials and Methods. To examine the effect of *dosR* expression in the  $\Delta$ *phoP* mutant, the mRNA levels of hypoxia-responsive *narG* and *nirB* were determined in the indicated strains by RT-qPCR analyses, as described in the legend to Fig. 1. (D) To verify the expression of PhoP and DosR in the indicated strains, mycobacterial cell extracts containing comparable amount of total proteins were resolved by SDS-PAGE, and the presence of the regulators was confirmed by Western blotting with anti-PhoP and anti-FLAG antibodies, respectively.

whereas *narG* and *nirB* were much less expressed in the mutant relative to the WT bacilli (Fig. 2A). This is consistent with reduced nitrogen scavenging by GlnR (34) and enhanced nitrite and nitrate reduction by the respective reductases (*nirB* and *narG*, respectively) (30) (see below). In contrast, (i) under identical conditions the *phoP* locus had no effect on the expression of *dosR*, *hspX*, and *nark2* (Fig. S2A) and (ii) under normoxia coupled with surplus ammonium chloride concentration, these genes were comparably expressed in WT and  $\Delta$ *phoP* mutant strains (Fig. 2B). On the other hand, regardless of the ammonium concentration, under normoxia the *phoP* locus had a striking effect on the expression of the hypoxia-responsive genes *dosR*, *hspX*, and *nark2* (Fig. S2B). Based on these results, we conclude that *phoP* plays a major regulatory role in mycobacterial nitrogen metabolism under oxygen-limiting (hypoxia) conditions. A regulatory scheme suggesting activation of *narG* and *nirB* and repression of *glnR* to lower nitrogen scavenging is shown in Fig. 2C.

**Regulation of hypoxia-responsive promoters by PhoP and DosR.** To examine PhoP-dependent *dosR* expression, we probed the PhoP binding site within the *dosR* promoter (dosRup, spanning positions –1438 to –774 relative to the start of the open reading frame [ORF]). Based on the knowledge of consensus PhoP binding site (32, 33) and more recent results on PhoP binding (24), we could locate a region spanning positions –1117 to –1100 within dosRup as the likely PhoP box. Next, mutant dosRup (dosRupmut) was generated by introducing mutations at the PhoP box, as shown in Fig. 3A, and transcriptional fusions of the WT (dosRup) and the mutant promoter (dosRupmut) were

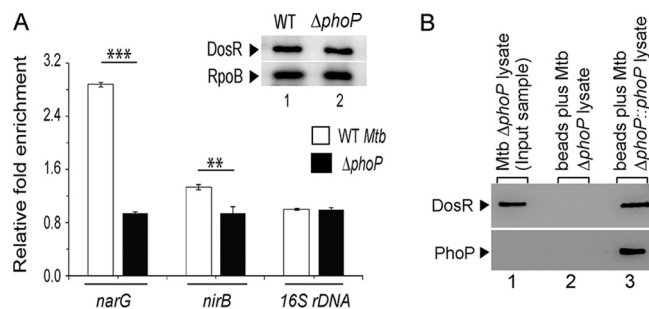


**FIG 4** Recruitment of PhoP and DosR within hypoxia-inducible promoters. (A) *In vivo* experiments compared the recruitment of DosR in WT and  $\Delta$ *phoP* strains grown under hypoxia. ChIP-qPCR experiments utilized anti-FLAG antibodies (Thermo Scientific) to determine the fold enrichments with respect to mock IP (without adding antibody) sample, as described in Materials and Methods, and the inset compares DosR expression in 10- $\mu$ g crude cell lysates; RpoB was used as the loading control. \*\*,  $P < 0.01$ ; \*,  $P < 0.05$ . (B) Crude cell lysates of  $\Delta$ *phoP* strains expressing His<sub>6</sub>-tagged PhoP (p19kpro-*phoP*) (Table S3) were incubated with Ni-NTA and eluted with 200 mM imidazole. Lane 1, input sample; lane 2, elution from the crude lysate of cells lacking *phoP* expression; lane 3, detection of DosR coelution with PhoP. The upper and lower panels identify DosR and PhoP by using anti-DosR and anti-His antibodies, respectively, and Western blotting as described in Materials and Methods.

cloned at the *Scal* site of pSM128 (35), a promoter-less integrative *lacZ* reporter vector with a streptomycin resistance gene. *M. tuberculosis* PhoP was expressed in *M. smegmatis* by using pME1mL1-*phoP* as described previously (36) (see Materials and Methods for details). Consistent with *phoP*-dependent activation of *dosR* expression (Fig. 1), the *dosRup-lacZ* fusion showed a significant activation [(4  $\pm$  0.9)-fold] of promoter activity with induction of *phoP* expression relative to the uninduced culture (Fig. 3B). However, *dosRupmut-lacZ* showed comparable  $\beta$ -galactosidase activity with or without induction of PhoP [a (1.2  $\pm$  0.05)-fold difference]. The inset image in Fig. 3B compares *M. tuberculosis* PhoP expression in *M. smegmatis* harboring WT or the mutant promoter. These results establish that PhoP-dependent activation of *dosR* expression involves the above-noted direct repeat motif as the primary target site of PhoP.

To examine whether *phoP*-dependent regulation of hypoxic response is achieved via DosR expression, we next expressed *dosR* in the *M. tuberculosis*  $\Delta$ *phoP* mutant and compared the expression levels of *narG* and *nirB* (Fig. 3C). The data unambiguously suggest that *narG* and *nirB* are significantly downregulated in a  $\Delta$ *phoP* mutant under normoxic growth conditions. Clearly, ectopic expression of DosR ( $\Delta$ *phoP-dosR*) was unable to restore *narG* and *nirB* expression, whereas the complemented  $\Delta$ *phoP* mutant ( $\Delta$ *phoP::phoP*) restored gene expression. These results suggest that activation of *narG* and *nirB* expression by PhoP is not attributable to PhoP dependent *dosR* activation under normoxia (Fig. 1A). Figure 3D confirms the expression of regulators in the indicated strains. From these results, we conclude that PhoP-dependent *dosR* expression cannot account for its regulation of hypoxic response. This observation fits well with the above finding that PhoP-dependent regulation of hypoxia-inducible genes (*dosR*, *hspX*, and *narK2*) is limited to normoxia only (Fig. 1) and thus possibly remain unlinked to the hypoxic response of *M. tuberculosis*.

Since both PhoP and DosR were shown to regulate hypoxia-responsive genes, we next compared the *in vivo* recruitment of DosR within hypoxia-responsive promoters of WT and  $\Delta$ *phoP* strains (Fig. 4A). This is because the hypoxia-responsive *narG*, *nirB*, and *glnR* genes showed a *phoP*-dependent expression during hypoxia (Fig. 1). Note that despite a comparable level of DosR in the WT and  $\Delta$ *phoP* strains under hypoxia (inset in Fig. 4A), we observed a significantly lower DosR recruitment, approximately 2- to 6-fold, within the target promoters in the  $\Delta$ *phoP* bacilli relative to the WT bacilli. Thus, the presence of PhoP is necessary for effective recruitment of DosR within the hypoxia-inducible promoters involved in mycobacterial N<sub>2</sub> metabolism. Notably, this finding is consistent with the previously reported *dosR*-dependent regulation of *narG* expression (13).

Considering these results, the recently reported PhoP-DosR interaction (24) emerged as a possible explanation for the regulation of hypoxia-inducible genes. To examine this, a whole-cell lysate of the  $\Delta phoP$  mutant expressing His-tagged PhoP, as described previously (37), was incubated with Ni-nitrilotriacetic acid (Ni-NTA), and proteins were eluted from an Ni-NTA column using imidazole (Fig. 4B). While the eluent showed clear presence of DosR (lane 3), we were unable to detect DosR from the cell lysate of the  $\Delta phoP$  mutant carrying the empty vector (p19Kpro) (lane 2; see Table S3). In agreement with the PhoP-DosR interaction recently reported by Vashist et al. (24), these results suggest a specific *in vivo* interaction between PhoP and DosR.

Next, we utilized a mycobacterial protein fragment complementation (M-PFC) assay to examine PhoP-DosR interaction using *M. smegmatis* as the surrogate host (Fig. S3) (see Table S3 for the plasmids used in this study). In agreement with results reported previously (24), our results also showed specific interaction between PhoP and DosR (Fig. S3A). However, under identical conditions, we were unable to detect interaction between PhoP and GlnR (Fig. S3B), suggesting that the regulation of *narG* and *nirB* expression during hypoxia is most likely GlnR independent. Using phosphorylation-defective mutants of PhoP and DosR (PhoPD71N and DosRD54N, respectively), we further showed that phosphorylation of the response regulators do not appear to influence PhoP-DosR protein-protein contacts (Fig. S3C and D).

**Probing PhoP-DosR protein-protein interactions.** To investigate interacting domains of PhoP and DosR, we next performed *in vitro* protein-protein interaction analysis using glutathione S-transferase (GST)-DosR and the domains of His<sub>6</sub>-tagged PhoP (Fig. 5A), previously shown to be functioning on their own (38). In pulldown assays, GST-DosR was immobilized on glutathione-Sepharose, followed by incubation with His<sub>6</sub>-tagged PhoP domains (Fig. 5A). Upon elution, PhoPN (comprising PhoP residues 1 to 141) (Fig. 5A, lane 1) is coeluted with GST-DosR from the bound glutathione-Sepharose by 10 mM glutathione (similar to PhoP [lane 4]). However, under identical conditions, none of the PhoP C domain constructs (PhoPC1 [comprising residues 141 to 247] or PhoPC2 [comprising residues 150 to 247]) is coeluted with GST-DosR (lanes 2 and 3).

To identify the corresponding interacting domain of DosR, we used GST-PhoP and His-tagged DosR domain constructs in pulldown assays similar to those described above (Fig. 5B; see Table S3). Interestingly, DosRN (comprising residues 1 to 193) coeluted with GST-PhoP (lane 1); however, DosRC (comprising residues 143 to 217) under identical conditions, did not coelute with GST-PhoP (lane 2), suggesting a specific interaction between DosRN and PhoP. Figure S4 shows the purified form of the recombinant regulators (and their domains) used in these experiments. Consistent with these results, *M. smegmatis* cells coexpressing PhoPN and DosR (Fig. 5C), as well as PhoP and DosRN (Fig. 5D), pairs grew well on trimethoprim (TRIM) plates. However, cells coexpressing PhoPC/DosR or PhoP/DosRC pairs failed to grow on TRIM plates (compare Fig. 5C and D). Note that all of these cells grew well on plates lacking TRIM. Together, these results suggest that the N domain of PhoP interacts with the N domain of DosR. Based on the promoter occupancy of PhoP (23, 32) and DosR (16, 39) and the orientation of the two interacting regulators, Fig. 5E summarizes a regulatory scheme showing coactivation of hypoxia-inducible genes (involved in N<sub>2</sub> metabolism) by PhoP and DosR.

**phoP-dependent growth restoration of *M. tuberculosis* under hypoxia.** With the results showing a striking impact of PhoP on expression of hypoxia-inducible genes involved in N<sub>2</sub> metabolism, we sought to examine growth of WT and  $\Delta phoP$  strains under hypoxia (Fig. 6). When compared under hypoxia coupled with N<sub>2</sub>-limiting conditions, both strains showed comparably limited growth (Fig. 6A). However, under hypoxia coupled with N<sub>2</sub> surplus conditions, WT bacilli showed significant growth restoration (Fig. 6B). In striking contrast, the *M. tuberculosis*  $\Delta phoP$  mutant strain under identical conditions failed to resume growth, as had the WT bacilli, and consistently showed a lower growth [(2 ± 0.1)-fold] relative to the WT bacilli. Importantly, growth

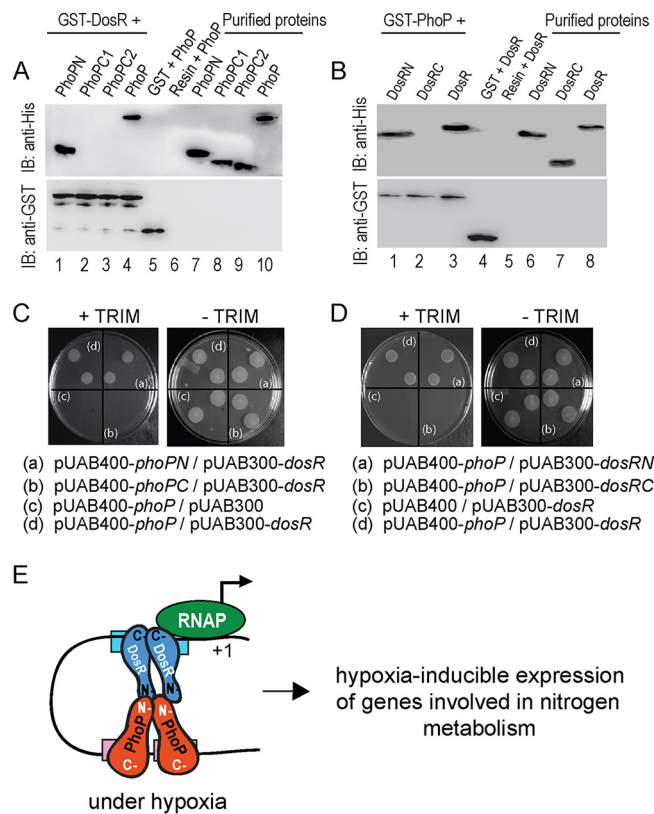


**FIG 5** Probing interacting domains of PhoP and DosR. (A) The indicated His<sub>6</sub>-tagged PhoP domains were incubated with glutathione-Sepharose, previously immobilized with GST-DosR. Fractions of bound proteins (lanes 1 to 4) were analyzed by anti-His (upper panel) or anti-GST antibody (lower panel). Control sets include GST alone (lane 5) or the resin alone (lane 6); lanes 7 to 10 resolve purified PhoP constructs. (B) Likewise, indicated His<sub>6</sub>-tagged DosR domains were incubated with glutathione-Sepharose previously immobilized with GST-PhoP. Fractions of bound proteins (lanes 1 to 3) were probed with anti-His or anti-GST antibody (as described above). Control sets include GST alone (lane 4) or the resin alone (lane 5); lanes 6 to 8 resolved purified DosR constructs. The results suggest that DosRN and not DosRC retains the ability to interact with PhoP. (C and D) M-PFC experiments examined interactions between the indicated PhoP domains and DosR (C) or between PhoP and indicated DosR domains (D), respectively, using the full-length PhoP/DosR pair as the positive control. (E) Model depicting how PhoP and DosR function as coactivators of hypoxia-inducible gene expression (right). While PhoP-DosR interaction via their received domains contributed to the additional stability of the transcription initiation complex, mycobacterial RNA polymerase bound to the target site of the promoter to initiate transcription.

defect of the  $\Delta$ *phoP* mutant could be restored to the WT level with the complementation of the mutant (see Fig. S5), underscoring the importance of *phoP* in utilizing an available nitrogen resource during hypoxia. As controls, under normoxia, the WT and  $\Delta$ *phoP* strains grew comparably well regardless of the available ammonium chloride concentration (Fig. 6C and D). We conclude that PhoP, under hypoxic conditions, integrates nitrogen metabolism and hypoxia.

## DISCUSSION

*M. tuberculosis*, during infection, survives in environments with oxygen-limiting conditions, and yet the mechanisms that promote survival of the metabolically inactive bacilli remain largely unknown. The fact that oxygen pressure within granulomas remains low (40, 41), yet reactivation from latency takes place within oxygen-rich sites of the lung, suggests that oxygen availability remains the key determinant. In keeping with this, mycobacterial growth both *in vitro* and *in vivo* is strongly influenced by the available oxygen pressure (2, 42), suggesting hypoxia as one of the major trigger factors of latency and reactivation.

Although hypoxia is known to increase nitrate reduction in *M. tuberculosis* (7), mechanism of regulation of nitrogen metabolism during oxygen austerity remained



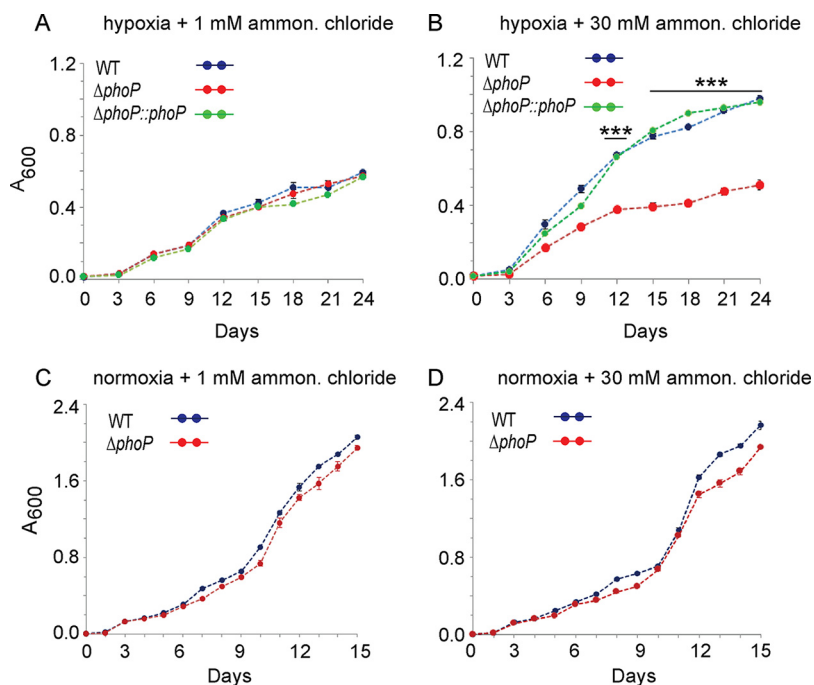


**FIG 6** Mycobacterial growth under hypoxia coupled with surplus or limited nitrogen availability. Growth curves of indicated strains were compared under hypoxia (A and B) or normoxia (C and D), coupled with either limiting nitrogen (1 mM  $\text{NH}_4\text{Cl}$ ) or surplus nitrogen (30 mM  $\text{NH}_4\text{Cl}$ ) conditions. The values represent averages from replicate experiments with standard deviations from at least three independent cultures (\*\*\*,  $P < 0.001$ ).

obscure. While DosR remains essential for *M. tuberculosis* adaptation and survival under hypoxic environment, PhoP coordinates pH homeostasis via regulation of pH-inducible gene expression. Interestingly, DosR was recently implicated in *M. tuberculosis* growth at low pH under anaerobic conditions (25). Thus, we sought to investigate role of PhoP on hypoxic response of *M. tuberculosis*. Results reported in this study suggest that PhoP activates expression of mycobacterial genes related to  $\text{N}_2$  metabolism under oxygen-limiting conditions with effective assistance from the hypoxia regulator DosR. Together, our results provide a new biological insight showing metabolic switching of *M. tuberculosis* in response to hypoxia by the convergence of two major response regulators.

It is noteworthy that *M. tuberculosis*, which evolved as an obligate human pathogen, has lost the majority of the regulatory pathways that are part of the metabolism of easily available nutrients. Thus, the nitrogen metabolism regulon is largely restricted to nitrite and nitrate reductases, making available the most likely nitrogen sources within the host (43). Notably, nitrate remains the final electron acceptor in lieu of oxygen to support growth of many bacteria during oxygen austerity. Therefore, hypoxia-induced nonreplicating persistence in *M. tuberculosis* is accompanied by nitrate reduction as a way to maintain redox balance and save the energy reservoir during downshift (8). In keeping with these results, under hypoxia, (i) activation of *nirBD* and *narGHJIJ* loci, which function in nitrite and nitrate reductions, respectively, and (ii) repression of *glnR*, which controls nitrogen scavenging (43) by the *phoP* locus, unravel a strikingly novel role of PhoP in nitrogen metabolism during hypoxia.

Considering the involvement of both the regulators, it was of interest to examine whether these two are functionally connected. Clearly, the recruitment of PhoP and DosR (Fig. 4), most likely controlled by protein-protein interactions (Fig. 4), regulates the activation of hypoxia-inducible genes and provides an integrated view of our results. Under such a situation, for a more effective functioning DosR recruitment is possibly ensured within target promoters already bound by PhoP. Based on the involvement of both regulators, coupled with our findings that the respective

N domains interact with each other (Fig. 5A to D), we propose a model (Fig. 5E) suggesting how PhoP-DosR interaction controls precise regulation of hypoxic response, a key step in the intracellular survival of *M. tuberculosis*. These considerations take on more significance in the light of previously identified PhoP and DosR binding sites within the aforementioned promoters. The arrangement and spacing between the binding sites are strongly indicative of DNA looping, possibly to assist transcription initiation. Together, these results (i) suggest a critical role of PhoP in binding and transcriptional control of *narG* and *nirB* and (ii) account for why DosR could not be recruited at these promoters in the  $\Delta$ *phoP* *M. tuberculosis* strain (Fig. 4B), a finding that fits well with the previously reported PhoP-DosR interaction data (24) (Fig. 4). Although the model (Fig. 5E) shows an equimolar PhoP and DosR in the ternary complex, there is no evidence to suggest 1:1 binding stoichiometry. However, as independent regulators, in both cases a dimer of PhoP or DosR has been shown to bind DNA (16, 23, 39). Based on the chromatin immunoprecipitation (ChIP) results (Fig. 4), DosR remains ineffective in the  $\Delta$ *phoP* mutant and therefore the  $\Delta$ *phoP* mutant is expected to display a growth defect under hypoxia. However, we found comparably limited growth by both the WT and the mutant bacteria under hypoxia (Fig. 6A). We argue that PhoP-DosR interaction-dependent regulation possibly controls a few critical genes related to nitrogen metabolism, and therefore a significant growth defect of the  $\Delta$ *phoP* mutant relative to the WT bacilli is apparent only when surplus nitrogen is available during oxygen austerity (Fig. 6B).

The integration of two signaling systems, either similar systems or systems of different types, has been shown in numerous other biological systems. An earlier study demonstrates the role of PknH in the phosphorylation of DosR, which is necessary for complete induction of the *M. tuberculosis* *dosR* regulon (44). Although these results suggest the convergence of two different types of signaling modules for a common function, along a similar line, DosR interacts with the housekeeping sigma factor SigA for bacterial survival under dormancy (18). Recently, we showed that PhoP interacts with the nucleoid-associated protein EspR to control ESAT-6 secretion (37). In the present study, we show that N domains that are phosphorylated for activation of respective regulators interact with each other (Fig. 5). This is in sharp contrast to recently reported PhoP-HspR and PhoP-HrcA interactions, where PhoPN was shown to interact with the C-terminal ends of mycobacterial heat shock repressors (45). Although the phosphorylation of either of the regulators does not seem to influence PhoP-DosR protein-protein contacts (see Fig. S3C and D in the supplemental material), the involvement of additional regulatory control by the N domains other than phosphorylation (Fig. 5), which enables appropriate *in vivo* functioning of the regulators via protein-protein contacts (Fig. 4), offers a new mechanistic insight. However, based on these results we cannot rule out the involvement of PhoR and DosS/DosT during hypoxia. In fact, a previous study suggests cross talk between the two signaling systems (46), suggesting that phosphorylation by a noncognate kinase(s) may even have *in vivo* significance. Given the facts that complex regulation of the level of phosphorylated DosR is determined by the balancing act of kinase/phosphatase functions of DosS (47) and that multiple signals are sensed by DosS and DosT (12, 14, 48, 49) to activate DosR, based on the results presented above we cannot completely exclude the possibility of the phosphorylation of DosR playing a role in PhoP-DosR interaction. Clearly, more experiments are needed to assess how specific stress conditions phosphorylate PhoP and DosR and coordinate their functioning to support mycobacterial survival in a phagosomal environment.

Since several examples establish that either two different or similar regulatory systems are often integrated toward a common regulatory function, integration via a single interaction (or lack thereof) possibly could have a large or a small impact on the transcriptional control of different target promoters. It is conceivable that a diversity of interactions at numerous promoters (belonging to various regulons) may significantly enhance the available combinations of potential regulatory interactions to fine-tune context-dependent gene expression. Since a hypoxic response

is believed to play a major role in dormancy adaptation, DosR activation is associated with metabolic changes where the tubercle bacilli move into a nonreplicating persistent state. Therefore, it is not too difficult to imagine that control mechanisms (for example, PhoP-DosR interactions) exist that interfere with bacterial persistence unless an appropriate signal is recognized. In fact, this is expected, since activation of the regulon consisting of ~48 genes would otherwise be energy demanding, and it therefore appears that a second molecular control system (in addition to DosS/DosT) is in place to regulate the induction of DosR only under the most appropriate stress conditions.

In conclusion, we have identified a signaling mechanism in *M. tuberculosis* that regulates hypoxia-inducible genes related to nitrogen metabolism. To our knowledge, this is the first report of a regulatory pathway that links the virulence regulator PhoP to the expression of nitrite and nitrate reductases under hypoxia. This study explains, at least in part, a fundamental mechanism of metabolic switching underlying how nitrogen metabolism genes are activated for survival of *M. tuberculosis* under oxygen austerity for a long period of time.

## MATERIALS AND METHODS

**Bacterial strains and culture conditions.** *E. coli* DH5 $\alpha$  and *E. coli* BL21(DE3) strains were grown at 37°C in Luria-Bertani medium containing appropriate antibiotics and used for cloning and for the overexpression of mycobacterial proteins, respectively. Although the  $\Delta$ phoP mutant and the complemented mutant have been described previously (31), the  $\Delta$ dosR mutant and the complemented mutant are also described below. *M. tuberculosis* strains were grown aerobically at 37°C in Middlebrook 7H9 liquid broth (containing 0.2% glycerol, 0.05% Tween 80, and 10% albumin-dextrose-catalase) or on 7H10 agar medium (containing 0.5% glycerol and 10% oleic acid-albumin-dextrose-catalase [OADC]). For growth under hypoxic conditions, stock cultures were aerobically subcultured twice to mid-log phase ( $A_{600}$  of 0.3 to 0.4) in Dubos (Difco) medium supplemented with 0.045% Tween 80, 10% albumin, and dextrose and subsequently inoculated into fresh medium at an  $A_{600}$  of 0.01. Oxyrase was used to remove excess oxygen, and 1.5  $\mu$ g/ml methylene blue was added as an indicator of oxygen depletion (7). *M. tuberculosis* growth under nitrogen excess or nitrogen-limiting conditions are as described previously (43), and the expression of *nirB* was measured by quantitative RT-PCR (RT-qPCR) using RNA from three independent cultures with *gapdh* as an internal control. Briefly, *M. tuberculosis* strains were grown as described above, washed twice in nitrogen-free Dubos medium, and inoculated in the same medium supplemented with either 1 mM (nitrogen limiting) or 30 mM (nitrogen surplus) ammonium chloride (Sigma). Transformation of WT and mutant *M. tuberculosis* strains and selection of transformants on appropriate antibiotics were carried out as described previously.

**RNA isolation and quantitative real-time RT-PCR.** Total RNA from *M. tuberculosis* was extracted as described previously (29) using exponentially growing bacterial cultures grown with or without stress. After extraction with chloroform-isoamyl alcohol, RNA was precipitated with chilled ethanol. Finally, RNA was treated with RNase-free DNase I (Invitrogen) for 20 min at room temperature to remove genomic DNA contamination. The integrity of the RNA samples was checked by determining the intactness of 23S and 16S rRNA using formaldehyde-agarose gel electrophoresis. RNA concentrations were determined by measuring the  $A_{260}$  and stored at  $-80^{\circ}\text{C}$ .

cDNA synthesis and PCRs using appropriate PAGE-purified primer pairs (200 nM) (see Table S1 in the supplemental material) were performed in an Applied Biosystems real-time PCR detection system using a Superscript III platinum-SYBR green one-step qRT-PCR kit (Invitrogen) and cycling conditions as described previously (29). For each pair of primers, a standard curve was generated using serially diluted RNA samples, and the PCR efficiency was evaluated. The average fold change in the expression of each sample relative to endogenously expressed *M. tuberculosis gapdh* (Rv1436) was calculated by the  $\Delta\Delta C_T$  method (50). Note that the  $C_T$  values for *gapdh* remained mostly unchanged under variable conditions of *M. tuberculosis* growth and that standard deviations were derived from at least three independent RNA preparations. Platinum Taq DNA polymerase (Invitrogen) was used to confirm absence of genomic DNA in our RNA preparations.

**Cloning.** Isolation and purification of nucleic acids, digestion with restriction enzymes, and analyses of nucleic acids or its fragments by agarose gel electrophoresis followed standard procedures. *M. tuberculosis* PhoP or its domain-specific overexpressing constructs have been described earlier (38). Likewise, the full-length DosR (encoding 654 bp) ORF and truncated DosR proteins (encoding the N-terminal 579 bp and C-terminal 222 bp of the *dosR* ORF) were cloned in T7-*lac*-based expression system pET28b (Novagen) as recombinant fusion proteins containing an N-terminal His<sub>6</sub> tag. The cloning strategy resulted in pET-*dosR*, pET-*dosRN*, and pET-*dosRC* comprising 217-amino-acid full-length DosR, 193-amino-acid DosRN (lacking the C-terminal 24 residues), and 74-residue DosRC (lacking the N-terminal 142 residues), respectively (51). Plasmid pGEX-*dosR* expressing DosR with an N-terminal glutathione S-transferase (GST) tag was generated by cloning PCR-derived *dosR* ORF fragment between BamHI and XhoI sites of pGEX 4T-1 (GE Healthcare) as described previously for pGEX-*phoP* (52). To complement *dosR* expression in the respective mycobacterial mutant, the ORF was cloned and expressed in the mycobacterial expression vector pSTKi (53). To express FLAG-tagged *dosR* in *M. tuberculosis*, the ORFs were cloned

and expressed in the mycobacterial expression vector p19Kpro (54). Point mutations in *phoP* and *dosR* genes were introduced by the two-stage overlap extension method and verified by DNA sequencing. The oligonucleotide primers used in cloning and construction of the plasmids are provided in Tables S2 and S3, respectively.

**Promoter regulation by *M. tuberculosis* PhoP in *M. smegmatis*.** *M. smegmatis* strains carrying indicated *lacZ* fusions and pME1mL1-*phoP*, expressing *M. tuberculosis* PhoP under the P<sub>myc1</sub>*tetO* promoter and the TetR repressor (or no expression plasmid as control), were grown either in absence or in the presence of 50 ng/ml anhydrotetracycline (ATc) as described previously (55). To determine promoter activity, cells from both induced and uninduced cultures were grown for 24 h, cell suspensions were sonicated, and the  $\beta$ -galactosidase activity of the extracts was determined. To assess TetR-dependent PhoP expression, crude cell lysates of *M. smegmatis* (~10  $\mu$ g of protein) were resolved by 12% SDS-PAGE and probed with anti-PhoP antibody (AlphaOmega Sciences, India).

**Proteins.** *M. tuberculosis* PhoP and its domains were expressed and purified as described previously (38). Full-length and truncated DosR proteins were expressed in *E. coli* BL21(DE3) as fusion proteins containing an N-terminal His<sub>6</sub> tag and purified by immobilized metal affinity chromatography (Ni-NTA; Qiagen). Full-length DosR was also expressed with N-terminal GST tag, as described for GST-PhoP (56). Finally, the proteins were stored in buffer containing 50 mM Tris-HCl (pH 7.9), 300 mM NaCl, and 10% glycerol. In all cases, the purity was verified by SDS-PAGE, and protein concentrations were determined by Bradford reagent with BSA as the standard, and expressed in equivalent of protein monomers.

**Immunoblotting.** Crude cell lysates of *M. tuberculosis* were resolved by 12% SDS-PAGE and visualized by Western blotting. For immunoblotting, resolved samples were electroblotted onto polyvinylidene difluoride (polyvinylidene difluoride) membranes (Millipore) and were detected by affinity-purified antibodies elicited in rabbit (AlphaOmega Sciences). RNA polymerase, used as a loading control, was detected by anti-RpoB (Abcam). Anti-His and anti-GST antibodies were from GE Healthcare. Goat anti-rabbit and goat anti-mouse secondary antibodies conjugated to horseradish peroxidase were procured from AlphaOmega Sciences, and blots were developed with Luminata Forte chemiluminescence reagent (Millipore).

**ChIP-qPCR.** *M. tuberculosis* was grown as described above and processed for ChIP experiments using purified anti-PhoP (Alpha Omega Sciences) or anti-FLAG (Thermo Scientific) antibody and protein A/G-agarose beads (Pierce) as described previously (57). qPCR was performed using PAGE purified primer pairs (Sigma) (Table S1) that spanned appropriate promoter regions of interest. PCR mix contained suitable dilutions of immunoprecipitation (IP) DNA in a reaction buffer containing SYBR green mix and specific primers (200 nM). An IP experiment without adding antibody (mock) served as a negative control, and data were normalized against PCR signal from a mock-treated sample. Typically, 40 cycles of amplification were carried out using an Applied Biosystems real-time PCR detection system with serially diluted DNA samples (mock, IP treated, and total input). Melting curve analysis was carried out to confirm amplification of a single product in all cases. Enrichment of PCR signal from anti-PhoP or anti-FLAG IP relative to the signal from an IP experiment without adding any antibody (mock) was measured to determine efficiency of recruitment. Specific PCR enrichment was ensured by performing ChIP-qPCR of the identical IP samples using *gapdh*/16S rRNA gene-specific primers. Each data point represents the mean of duplicate qPCR measurements using at least three independent *M. tuberculosis* cultures.

**Mycobacterial protein fragment complementation assays.** To express *M. tuberculosis* PhoP or its domains in *M. smegmatis*, *phoP* and/or its appropriate domain constructs were cloned in the integrative vector pUAB400 (Kan<sup>r</sup>) (Table S3) between MfeI and HindIII sites, as described previously (56). Similarly, *dosR*, *glnR*, and truncated *dosR* ORFs were cloned in episomal plasmid pUAB300 (Hyg<sup>r</sup>) (Table S3) between BamHI/HindIII sites to generate pUAB300-*dosR*, pUAB-*glnR*, pUAB300-*dosRN*, and pUAB300-*dosRC*, respectively. Next, cotransformed cells were selected on 7H10/Kan/Hyg plates in the absence or presence of 15  $\mu$ g/ml trimethoprim (TRIM; Sigma), as described previously (58). In this assay, two interacting proteins as separate fusion constructs of two domains of murine dihydrofolate reductase (mDHFR) when coexpressed in *M. smegmatis* reconstitute functional mDHFR and enable the bacteria to grow on medium containing TRIM. As a positive control, ESAT-6/CFP-10-expressing constructs were used in the M-PFC experiments. Note that all of the strains used in this study grew well in the absence of TRIM.

## SUPPLEMENTAL MATERIAL

Supplemental material for this article is available online only.

**SUPPLEMENTAL FILE 1**, PDF file, 0.5 MB.

## ACKNOWLEDGMENTS

We thank Adrie Steyn for pUAB300 and pUAB400 plasmids, G. Marcela Rodriguez and Issar Smith for the  $\Delta$ *phoP* and complemented mutant strains, Harsh Goar for purification of recombinant DosR, and Ashwani Kumar for very helpful discussions.

This study was supported by a research grant (to D.S.) from the SERB-Department of Science and Technology (DST; EMR/2016/004904), Government of India, and by intramural funding from CSIR-IMTECH. P.R.S. and V.A.K. received financial support from DST and CSIR, respectively.

The funders had no role in the study design, data collection and interpretation, or the decision to submit the work for publication.

## REFERENCES

- Nathan C, Shiloh MU. 2000. Reactive oxygen and nitrogen intermediates in the relationship between mammalian hosts and microbial pathogens. *Proc Natl Acad Sci U S A* 97:8841–8848. <https://doi.org/10.1073/pnas.97.16.8841>.
- Rustad TR, Sherrid AM, Minch KJ, Sherman DR. 2009. Hypoxia: a window into *Mycobacterium tuberculosis* latency. *Cell Microbiol* 11:1151–1159. <https://doi.org/10.1111/j.1462-5822.2009.01325.x>.
- Wayne LG, Sohaskey CD. 2001. Nonreplicating persistence of mycobacterium tuberculosis. *Annu Rev Microbiol* 55:139–163. <https://doi.org/10.1146/annurev.micro.55.1.139>.
- Mishra BB, Rathinam VA, Martens GW, Martinot AJ, Kornfeld H, Fitzgerald KA, Sasseti CM. 2013. Nitric oxide controls the immunopathology of tuberculosis by inhibiting NLRP3 inflammasome-dependent processing of IL-1 $\beta$ . *Nat Immunol* 14:52–60. <https://doi.org/10.1038/ni.2474>.
- Nicholson S, Bonecini-Almeida MG, Lapa e Silva JR, Nathan C, Xie QW, Mumford R, Weidner JR, Calaycay J, Geng J, Boechat N, Linhares C, Rom W, Ho JL. 1996. Inducible nitric oxide synthase in pulmonary alveolar macrophages from patients with tuberculosis. *J Exp Med* 183:2293–2302. <https://doi.org/10.1084/jem.183.5.2293>.
- Choi HS, Rai PR, Chu HW, Cool C, Chan ED. 2002. Analysis of nitric oxide synthase and nitrotyrosine expression in human pulmonary tuberculosis. *Am J Respir Crit Care Med* 166:178–186. <https://doi.org/10.1164/rccm.2201023>.
- Sohaskey CD, Wayne LG. 2003. Role of *narK2X* and *narGHJ* in hypoxic upregulation of nitrate reduction by *Mycobacterium tuberculosis*. *J Bacteriol* 185:7247–7256. <https://doi.org/10.1128/jb.185.24.7247-7256.2003>.
- Wayne LG, Hayes LG. 1998. Nitrate reduction as a marker for hypoxic shift-down of *Mycobacterium tuberculosis*. *Tuberc Lung Dis* 79:127–132. <https://doi.org/10.1054/tuld.1998.0015>.
- Wayne LG, Doubek JR. 1965. Classification and identification of mycobacteria. II. Tests employing nitrate and nitrite as substrate. *Am Rev Respir Dis* 91:738–745.
- Rachman H, Strong M, Ulrichs T, Grode L, Schuchhardt J, Mollenkopf H, Kosmiadi GA, Eisenberg D, Kaufmann SH. 2006. Unique transcriptome signature of *Mycobacterium tuberculosis* in pulmonary tuberculosis. *Infect Immun* 74:1233–1242. <https://doi.org/10.1128/IAI.74.2.1233-1242.2006>.
- Fenhalls G, Stevens L, Moses L, Bezuidenhout J, Betts JC, Helden Pv P, Lukey PT, Duncan K. 2002. In situ detection of *Mycobacterium tuberculosis* transcripts in human lung granulomas reveals differential gene expression in necrotic lesions. *Infect Immun* 70:6330–6338. <https://doi.org/10.1128/iai.70.11.6330-6338.2002>.
- Voskuil MI, Schnappinger D, Visconti KC, Harrell MI, Dolganov GM, Sherman DR, Schoolnik GK. 2003. Inhibition of respiration by nitric oxide induces a *Mycobacterium tuberculosis* dormancy program. *J Exp Med* 198:705–713. <https://doi.org/10.1084/jem.20030205>.
- Park HD, Guinn KM, Harrell MI, Liao R, Voskuil MI, Tompa M, Schoolnik GK, Sherman DR. 2003. Rv3133c/dosR is a transcription factor that mediates the hypoxic response of *Mycobacterium tuberculosis*. *Mol Microbiol* 48:833–843. <https://doi.org/10.1046/j.1365-2958.2003.03474.x>.
- Ioanoviciu A, Meharena YT, Poulos TL, Ortiz de Montellano PR. 2009. DevS oxy complex stability identifies this heme protein as a gas sensor in *Mycobacterium tuberculosis* dormancy. *Biochemistry* 48:5839–5848. <https://doi.org/10.1021/bi802309y>.
- Saini DK, Malhotra V, Dey D, Pant N, Das TK, Tyagi JS. 2004. DevR-DevS is a bona fide two-component system of *Mycobacterium tuberculosis* that is hypoxia-responsive in the absence of the DNA-binding domain of DevR. *Microbiology* 150:865–875. <https://doi.org/10.1099/mic.0.26218-0>.
- Chauhan S, Tyagi JS. 2008. Cooperative binding of phosphorylated DevR to upstream sites is necessary and sufficient for activation of the Rv3134c-devR operon in *Mycobacterium tuberculosis*: implication in the induction of DevR target genes. *J Bacteriol* 190:4301–4312. <https://doi.org/10.1128/JB.01308-07>.
- Chauhan S, Tyagi JS. 2009. Powerful induction of divergent tgs1-Rv3131 genes in *Mycobacterium tuberculosis* is mediated by DevR interaction with a high-affinity site and an adjacent cryptic low-affinity site. *J Bacteriol* 191:6075–6081. <https://doi.org/10.1128/JB.00310-09>.
- Gautam US, Sikri K, Vashist A, Singh V, Tyagi JS. 2014. Essentiality of DevR/DosR interaction with SigA for the dormancy survival program in *Mycobacterium tuberculosis*. *J Bacteriol* 196:790–799. <https://doi.org/10.1128/JB.01270-13>.
- Gonzalo-Asensio J, Maia C, Ferrer NL, Barilone N, Laval F, Soto CY, Winter N, Daffe M, Gicquel B, Martin C, Jackson M. 2006. The virulence-associated two-component PhoP-PhoR system controls the biosynthesis of polyketide-derived lipids in *Mycobacterium tuberculosis*. *J Biol Chem* 281:1313–1316. <https://doi.org/10.1074/jbc.C500388200>.
- Gonzalo-Asensio J, Mostowy S, Harders-Westerveen J, Huygen K, Hernández-Pando R, Thole J, Behr M, Gicquel B, Martin C. 2008. PhoP: a missing piece in the intricate puzzle of *Mycobacterium tuberculosis* virulence. *PLoS One* 3:e3496. <https://doi.org/10.1371/journal.pone.0003496>.
- Ryndak M, Wang S, Smith I. 2008. PhoP, a key player in *Mycobacterium tuberculosis* virulence. *Trends Microbiol* 16:528–534. <https://doi.org/10.1016/j.tim.2008.08.006>.
- Galagan JE, Minch K, Peterson M, Lyubetskaya A, Azizi E, Sweet L, Gomes A, Rustad T, Dolganov G, Glotova I, Abeel T, Mahwinney C, Kennedy AD, Allard R, Brabant W, Krueger A, Jaini S, Honda B, Yu WH, Hickey MJ, Zucker J, Garay C, Weiner B, Sisk P, Stolte C, Winkler JK, Van de Peer Y, Iazzetti P, Camacho D, Dreyfuss J, Liu Y, Dorhoi A, Mollenkopf HJ, Drogaris P, Lamontagne J, Zhou Y, Piquenot J, Park ST, Raman S, Kaufmann SH, Mohny RP, Chelsky D, Moody DB, Sherman DR, Schoolnik GK. 2013. The *Mycobacterium tuberculosis* regulatory network and hypoxia. *Nature* 499:178–183. <https://doi.org/10.1038/nature12337>.
- He X, Wang S. 2014. DNA consensus sequence motif for binding response regulator PhoP, a virulence regulator of *Mycobacterium tuberculosis*. *Biochemistry* 53:8008–8020. <https://doi.org/10.1021/bi501019u>.
- Vashist A, Malhotra V, Sharma G, Tyagi JS, Clark-Curtiss JE. 2018. Interplay of PhoP and DevR response regulators defines expression of the dormancy regulon in virulent *Mycobacterium tuberculosis*. *J Biol Chem* 293:16413–16425. <https://doi.org/10.1074/jbc.RA118.004331>.
- Reichlen MJ, Leistikow RL, Scobey MS, Born SEM, Voskuil MI. 2017. Anaerobic *Mycobacterium tuberculosis* cell death stems from intracellular acidification mitigated by the DosR regulon. *J Bacteriol* 199:e00320-17. <https://doi.org/10.1128/JB.00320-17>.
- Abramovitch RB, Rohde KH, Hsu FF, Russell DG. 2011. *aprABC*: a *Mycobacterium tuberculosis* complex-specific locus that modulates pH-driven adaptation to the macrophage phagosome. *Mol Microbiol* 80:678–694. <https://doi.org/10.1111/j.1365-2958.2011.07601.x>.
- Baker JJ, Johnson BK, Abramovitch RB. 2014. Slow growth of *Mycobacterium tuberculosis* at acidic pH is regulated by *phoPR* and host-associated carbon sources. *Mol Microbiol* 94:56–69. <https://doi.org/10.1111/mmi.12688>.
- Tan S, Sukumar N, Abramovitch RB, Parish T, Russell DG. 2013. *Mycobacterium tuberculosis* responds to chloride and pH as synergistic cues to the immune status of its host cell. *PLoS Pathog* 9:e1003282. <https://doi.org/10.1371/journal.ppat.1003282>.
- Bansal R, Anil Kumar V, Sevalkar RR, Singh PR, Sarkar D. 2017. *Mycobacterium tuberculosis* virulence-regulator PhoP interacts with alternative sigma factor SigE during acid-stress response. *Mol Microbiol* 104:400–411. <https://doi.org/10.1111/mmi.13635>.
- Malm S, Tiffert Y, Micklinghoff J, Schultze S, Joost I, Weber I, Horst S, Ackermann B, Schmidt M, Wohlleben W, Ehlers S, Geffers R, Reuther J, Bange FC. 2009. The roles of the nitrate reductase NarGHJ, the nitrite reductase NirBD and the response regulator GlnR in nitrate assimilation of *Mycobacterium tuberculosis*. *Microbiology* 155:1332–1339. <https://doi.org/10.1099/mic.0.023275-0>.
- Walters SB, Dubnau E, Kolesnikova I, Laval F, Daffe M, Smith I. 2006. The *Mycobacterium tuberculosis* PhoPR two-component system regulates genes essential for virulence and complex lipid biosynthesis. *Mol Microbiol* 60:312–330. <https://doi.org/10.1111/j.1365-2958.2006.05102.x>.
- Solans L, Gonzalo-Asensio J, Sala C, Benjak A, Uplekar S, Rougemont J, Guillhot C, Malaga W, Martin C, Cole ST. 2014. The PhoP-dependent ncRNA Mcr7 modulates the TAT secretion system in *Mycobacterium tuberculosis*. *PLoS Pathog* 10:e1004183. <https://doi.org/10.1371/journal.ppat.1004183>.

33. He X, Wang L, Wang S. 2016. Structural basis of DNA sequence recognition by the response regulator PhoP in *Mycobacterium tuberculosis*. *Clin Rep* 6:24442. <https://doi.org/10.1038/srep24442>.
34. Jenkins VA, Barton GR, Robertson BD, Williams KJ. 2013. Genome-wide analysis of the complete GlnR nitrogen-response regulon in *Mycobacterium smegmatis*. *BMC Genomics* 14:301. <https://doi.org/10.1186/1471-2164-14-301>.
35. Dussurget O, Timm J, Gomez M, Gold B, Yu S, Sabol SZ, Holmes RK, Jacobs WR, Jr, Smith I. 1999. Transcriptional control of the iron-responsive *fbxA* gene by the mycobacterial regulator IdeR. *J Bacteriol* 181:3402–3408. <https://doi.org/10.1128/JB.181.11.3402-3408.1999>.
36. Ehrt S, Guo XV, Hickey CM, Ryou M, Monteleone M, Riley LW, Schnappinger D. 2005. Controlling gene expression in mycobacteria with anhydrotetracycline and Tet repressor. *Nucleic Acids Res* 33:e21. <https://doi.org/10.1093/nar/gni013>.
37. Anil Kumar V, Goyal R, Bansal R, Singh N, Sevalkar RR, Kumar A, Sarkar D. 2016. EspR-dependent ESAT-6 protein secretion of *Mycobacterium tuberculosis* requires the presence of virulence regulator PhoP. *J Biol Chem* 291:19018–19030. <https://doi.org/10.1074/jbc.M116.746289>.
38. Pathak A, Goyal R, Sinha A, Sarkar D. 2010. Domain structure of virulence-associated response regulator PhoP of *Mycobacterium tuberculosis*: role of the linker region in regulator-promoter interaction(s). *J Biol Chem* 285:34309–34318. <https://doi.org/10.1074/jbc.M110.135822>.
39. Chauhan S, Tyagi JS. 2008. Interaction of DevR with multiple binding sites synergistically activates divergent transcription of narK2-Rv1738 genes in *Mycobacterium tuberculosis*. *J Bacteriol* 190:5394–5403. <https://doi.org/10.1128/JB.00488-08>.
40. Tsai MC, Chakravarty S, Zhu G, Xu J, Tanaka K, Koch C, Tufariello J, Flynn J, Chan J. 2006. Characterization of the tuberculous granuloma in murine and human lungs: cellular composition and relative tissue oxygen tension. *Cell Microbiol* 8:218–232. <https://doi.org/10.1111/j.1462-5822.2005.00612.x>.
41. Via LE, Lin PL, Ray SM, Carrillo J, Allen SS, Eum SY, Taylor K, Klein E, Manjunatha U, Gonzales J, Lee EG, Park SK, Raleigh JA, Cho SN, McMurray DN, Flynn JL, Barry CE, III. 2008. Tuberculous granulomas are hypoxic in guinea pigs, rabbits, and nonhuman primates. *Infect Immun* 76:2333–2340. <https://doi.org/10.1128/IAI.01515-07>.
42. Wayne LG. 1977. Synchronized replication of *Mycobacterium tuberculosis*. *Infect Immun* 17:528–530. <https://doi.org/10.1128/IAI.17.3.528-530.1977>.
43. Williams KJ, Jenkins VA, Barton GR, Bryant WA, Krishnan N, Robertson BD. 2015. Deciphering the metabolic response of *Mycobacterium tuberculosis* to nitrogen stress. *Mol Microbiol* 97:1142–1157. <https://doi.org/10.1111/mmi.13091>.
44. Chao JD, Papavinasasundaram KG, Zheng X, Chavez-Steenbock A, Wang X, Lee GQ, Av-Gay Y. 2010. Convergence of Ser/Thr and two-component signaling to coordinate expression of the dormancy regulon in *Mycobacterium tuberculosis*. *J Biol Chem* 285:29239–29246. <https://doi.org/10.1074/jbc.M110.132894>.
45. Sevalkar RR, Arora D, Singh PR, Singh R, Nandicoori VK, Karthikeyan S, Sarkar D, Sevalkar RR, Arora D, Singh PR, Singh R, Nandicoori VK, Karthikeyan S, Sarkar D. 2019. Functioning of mycobacterial heat shock repressors requires the master virulence regulator PhoP. *J Bacteriol* 201:e00013-19.
46. Agrawal R, Pandey A, Rajankar MP, Dixit NM, Saini DK. 2015. The two-component signalling networks of *Mycobacterium tuberculosis* display extensive cross-talk *in vitro*. *Biochem J* 469:121–134. <https://doi.org/10.1042/BJ20150268>.
47. Kaur K, Kumari P, Sharma S, Sehgal S, Tyagi JS. 2016. DevS/DosS sensor is bifunctional and its phosphatase activity precludes aerobic DevR/DosR regulon expression in *Mycobacterium tuberculosis*. *FEBS J* 283:2949–2962. <https://doi.org/10.1111/febs.13787>.
48. Kumar A, Toledo JC, Patel RP, Lancaster JR, Jr, Steyn AJ. 2007. *Mycobacterium tuberculosis* DosS is a redox sensor and DosT is a hypoxia sensor. *Proc Natl Acad Sci U S A* 104:11568–11573. <https://doi.org/10.1073/pnas.0705054104>.
49. Vos MH. 2008. Ultrafast dynamics of ligands within heme proteins. *Biochim Biophys Acta* 1777:15–31. <https://doi.org/10.1016/j.bbabi.2007.10.004>.
50. Schmittgen TD, Livak KJ. 2008. Analyzing real-time PCR data by the comparative  $C_T$  method. *Nat Protoc* 3:1101–1108. <https://doi.org/10.1038/nprot.2008.73>.
51. Gautam US, Chauhan S, Tyagi JS. 2011. Determinants outside the DevR C-terminal domain are essential for cooperativity and robust activation of dormancy genes in *Mycobacterium tuberculosis*. *PLoS One* 6:e16500. <https://doi.org/10.1371/journal.pone.0016500>.
52. Gupta S, Pathak A, Sinha A, Sarkar D. 2009. *Mycobacterium tuberculosis* PhoP recognizes two adjacent direct-repeat sequences to form head-to-head dimers. *J Bacteriol* 191:7466–7476. <https://doi.org/10.1128/JB.00669-09>.
53. Parikh A, Kumar D, Chawla Y, Kurthkoti K, Khan S, Varshney U, Nandicoori VK. 2013. Development of a new generation of vectors for gene expression, gene replacement, and protein-protein interaction studies in mycobacteria. *Appl Environ Microbiol* 79:1718–1729. <https://doi.org/10.1128/AEM.03695-12>.
54. De Smet KA, Kempell KE, Gallagher A, Duncan K, Young DB. 1999. Alteration of a single amino acid residue reverses fosfomycin resistance of recombinant MurA from *Mycobacterium tuberculosis*. *Microbiology* 145:3177–3184. <https://doi.org/10.1099/00221287-145-11-3177>.
55. Goyal R, Das AK, Singh R, Singh PK, Korpole S, Sarkar D. 2011. Phosphorylation of PhoP protein plays direct regulatory role in lipid biosynthesis of *Mycobacterium tuberculosis*. *J Biol Chem* 286:45197–45208. <https://doi.org/10.1074/jbc.M111.307447>.
56. Singh R, Anil Kumar V, Das AK, Bansal R, Sarkar D. 2014. A transcriptional co-repressor regulatory circuit controlling the heat-shock response of *Mycobacterium tuberculosis*. *Mol Microbiol* 94:450–465. <https://doi.org/10.1111/mmi.12778>.
57. Fol M, Chauhan A, Nair NK, Maloney E, Moomey M, Jagannath C, Madiraju MV, Rajagopalan M. 2006. Modulation of *Mycobacterium tuberculosis* proliferation by MtrA, an essential two-component response regulator. *Mol Microbiol* 60:643–657. <https://doi.org/10.1111/j.1365-2958.2006.05137.x>.
58. Singh A, Mai D, Kumar A, Steyn AJ. 2006. Dissecting virulence pathways of *Mycobacterium tuberculosis* through protein-protein association. *Proc Natl Acad Sci U S A* 103:11346–11351. <https://doi.org/10.1073/pnas.0602817103>.